Table of Contents

Supplementary Methods

Lipidomics analysis

Lipid composition analysis

Extracellular carbohydrate characterization

TEM characterization and lattice-plane assignment

TEA and LCA analysis

Supplementary Tables

Supplementary Table S1. Strains used in this study

Supplementary Table S2. Plasmids used in this study

Supplementary Table S3. Main primers used in this study

Supplementary Table S4. Genes overexpressed or knocked out in this study

Supplementary Table S5. Synthesized genes used in this study

Supplementary Table S6. SgRNA sequences and genomic integration sites used in this study

Supplementary Table S7. Reference genomes used for transcriptomic analysis of six different strains

Supplementary Table S8. Comparison of kinetic parameters of ACS activity among different microorganisms

Supplementary Table S9. Design of ^{13}C isotope-tracing experiments for 3-HP biosynthesis

Supplementary Table S10. Comparison of representative microbial platforms for high-titer 3-HP production

Supplementary Table S11. The biohybrid systems integrating chemical CO_2 or CO reduction with biological synthesis to produce value-added products

Supplementary Table S12. Assumptions for the 3-HP production from CO_2-derived ethanol

Supplementary Table S13. n^{th}-plant assumptions required by techno-economic analysis

Supplementary Table S14. Capital expenditures for the annual production of 5,000-ton 3-HP from CO_2

Supplementary Table S15. Operating expenditures for the annual production of 5,000-ton 3-HP from CO_2

Supplementary Table S16. Global warming potential for producing 1 kg of 3-HP

Supplementary Table S17. Definitions and evaluation criteria for the substrate comparison in Fig. 1a

Supplementary Figures

Supplementary Figure S1. Screening of endogenous promoters driving eGFP expression in *K. phaffii* under ethanol-based growth

Supplementary Figure S2. Detailed process design for CO_2-derived ethanol conversion to 3-HP

References

Supplementary Methods

Lipidomics analysis

LT-13 and LT-28 cells were collected using the same cultivation and sampling procedures as those used for the proteomic and metabolomic analyses, with six biological replicates for each strain. Lipids were extracted from approximately 50 mg of cell samples using methanol/water (2:5, v/v) and methyl tert-butyl ether (MTBE). Non-targeted lipidomics was performed using a Vanquish UHPLC system coupled to a Q Exactive HF-X mass spectrometer (Thermo Fisher Scientific) equipped with an Accucore C30 column (100 mm × 2.1 mm, 2.6 μm). Mass spectra were acquired in both positive- and negative-ion modes. Raw data were processed using LipidSearch (Thermo Fisher Scientific) for peak detection, alignment and lipid annotation. Lipid features were sum-normalized and log10-transformed after filtering features with >30% relative standard deviation in quality-control samples. Principal component analysis (PCA) and orthogonal partial least-squares discriminant analysis (OPLS-DA) were performed using the R package ropls (v.1.6.2). Differential lipid species were defined by a two-sided unpaired Student's *t*-test ($P < 0.05$) and a variable importance in projection (VIP) score >1 derived from the OPLS-DA model.

Lipid composition analysis

Membrane lipid metrics were calculated from normalized lipid abundances. Average acyl-chain length (ACL) and unsaturation index (UI) were calculated for phospholipids (PC, PE, PI, PS, PG, PA and CL) as abundance-weighted averages of the number of carbon atoms and double bonds per acyl chain, respectively. The PC/PE ratio was calculated from the summed abundances of phosphatidylcholine and phosphatidylethanolamine species, and the Cer/PL ratio was calculated as the summed abundance of ceramide species relative to total phospholipids (PC, PE, PI, PS, PG, PA and CL). Metrics were calculated independently for each biological replicate (n = 6), and comparisons between LT-13 and LT-28 were performed using two-sided Welch's *t*-tests (Extended Data Fig. 7a).

Extracellular carbohydrate characterization

Total carbohydrate content in cell-free fermentation supernatants from strain LT-28 was quantified using the anthrone-sulfuric acid colorimetric assay. For detailed compositional and molecular-size profiling, identical cell-free fermentation supernatant samples were submitted for contract analytical services at Yangzhou BoRui Saccharide Biotech Co., Ltd (Yangzhou, China). Two complementary HPAEC-PAD (high-performance anion-exchange chromatography with pulsed amperometric detection) measurements were performed: free

monosaccharide analysis (direct injection without acid hydrolysis), and total-monosaccharide analysis after trifluoroacetic-acid (TFA) hydrolysis. For TFA hydrolysis, 1 mL supernatant was mixed with 2 mL of 3 M TFA and incubated at 120 °C for 3 h. Hydrolysates were dried under nitrogen flow, re-dissolved, diluted, centrifuged, and filtered through a 0.22 μm membrane prior to HPAEC-PAD injection on a Dionex CarboPac TM PA20 column (3 mm × 150 mm, ThermoFisher). Elution gradients, standards and quantification followed the provider-established workflow.

High-performance gel-permeation chromatography (HPGPC) was applied to determine molecular-size distribution of carbohydrate species in the same supernatant. The system (Thermo U3000) was equipped with a refractive-index detector (Shimadzu RI-20A) and tandem BRT105-103-101 gel columns (8 mm × 300 mm). The mobile phase was 0.2 M NaCl at a flow rate of 0.7 mL/min, column temperature 40 °C. A series of pullulan standards and maltoheptaose were used for calibration to obtain peak molecular mass (Mp), weight-average molecular mass (Mw), number-average molecular mass (Mn). Peak-area percentages from refractive-index chromatograms were used to describe molecular-size fractions.

To calculate intrinsic monosaccharide-residue molar percentages of secreted oligo- and poly-saccharide fractions, free monosaccharide concentrations obtained from direct-injection HPAEC-PAD were subtracted from total monosaccharide concentrations measured after TFA hydrolysis. The resulting values represent monosaccharides released exclusively upon glycosidic-bond cleavage of oligo- and polysaccharides. Molar fractions were computed based on corresponding monosaccharide molar masses.

TEM characterization and lattice-plane assignment

For TEM analysis, catalyst powders were dispersed in ethanol by ultrasonication for 5 min, and the supernatant was drop-cast onto molybdenum grids. TEM and HRTEM images were acquired using a Talos F200X G2 field-emission transmission electron microscope operated at 200 kV. HRTEM images were analysed using DigitalMicrograph software; selected regions containing well-resolved lattice fringes were subjected to fast Fourier transform (FFT) analysis and inverse FFT reconstruction. Interplanar spacings were determined from intensity profiles perpendicular to the lattice fringes by averaging approximately 10 consecutive lattice periods and were assigned to the corresponding crystallographic planes by comparison with standard PDF values together with the XRD phase-identification results. EDS elemental mapping was performed on the same Talos F200X G2 instrument at 200 kV to determine the spatial distribution of constituent elements in the catalysts.

TEA and LCA analysis

Process simulation. A schematic depicting the generation of 3-HP from a CO2-derived ethanol process is shown in Fig.7c. This study entailed the design of a 3-HP production process using Aspen Plus v14 software, which was utilized to conduct calculations for mass and energy balance. The 3-HP manufacturing process consisted of five components: ethanol production (A100), 3-HP production (A200), 3-HP purification (A300), tail Gas treatment and utilities (A400-A500). The principal assumptions of Aspen Plus v14 are presented for M1. The assumptions of the whole process are illustrated in Supplementary Table 12 and Table 13. The detailed procedure for the techno-economic analysis (TEA) of 3-HP production from CO_2 is described as follows:

①Ethanol production (A100). Ethanol was produced through the conversion of CO_2 and hydrogen (H_2) into ethanol. At a pressure of 3.0 MPa, an H_2:CO_2 molar ratio of 3:1, and a reaction temperature of 320 °C, the process achieved a single-pass CO_2 conversion of over 26.1%, with a CO_2 selectivity of 25.4%.

$2CO_2 + 6H_2 \rightarrow 2CH_3OH + 2H_2O$

$H_2 + CO_2 \rightarrow CO + H_2O$

$CO_2 + 4H_2 \rightarrow CH_4 + 2H_2O$

$CO_2 + 3H_2 \rightarrow CH_3OH + H_2O$

$2CO_2 + 5H_2 \rightarrow CH_3CHO + 3H_2O$

$2CO_2 + 4H_2 \rightarrow CH_3COOH + 2H_2O$

$2CO_2 + 7H_2 \rightarrow C_2H_6 + 4H_2O$

The off-gases generated during ethanol production were subsequently treated in the tail-gas treatment and recycling unit. Unreacted H_2 and CO_2 were recovered from the off-gas stream and recycled to the ethanol synthesis section, while the remaining combustible gases were directed to the combined heat and power (CHP) unit for energy recovery. The make-up hydrogen required for thermocatalytic ethanol production was supplied as externally purchased low-carbon hydrogen, with by-product-derived hydrogen adopted as the reference hydrogen source (https://www.h2-tech.com/articles/2026/march-2026/advanced-h2-production/the-low-carbon-h2-from-byproduct-recovery/). All externally supplied electricity used in the Aspen Plus simulation was assumed to be generated from solar photovoltaic power.

②3-HP production (A200). 3-HP production (A200). The 3-HP production process was modeled based on the de novo biosynthesis of 3-HP by the engineered K. phaffii engineered

strain LT-28, using ethanol as the primary carbon and energy source and CO_2 as a co-substrate. In Aspen Plus, the complex intracellular metabolic network was simplified into overall stoichiometric reactions to enable process-level mass and energy balance calculations. The reactions accounting for 3-HP formation, biomass synthesis, and ethanol oxidation were defined as follows:

Ethanol + CO_2 → 3-HP

2Ethanol + 1.75O_2 + NH_3 → Biomass + 3.5H_2O

Ethanol + 3O_2 → 2CO_2 + 3H_2O

Biomass＝$C_4H_8O_2N$

③3-HP purification (A300). The downstream separation and purification process for 3-HP was modeled based on the experimentally validated process reported by Mahata et al. Briefly, the fermentation broth was first subjected to centrifugation for biomass removal, followed by activated-carbon treatment for decolorization and removal of residual organic impurities. The clarified broth was subsequently treated using sequential cation- and anion-exchange steps to remove ionic impurities, including ammonium, metal ions, sulfate and chloride. The 3-HP-rich stream obtained after ion exchange was then concentrated by evaporation to produce a 30% (w/v) aqueous 3-HP solution[1].

In the Aspen Plus simulation, the experimentally reported stepwise 3-HP recoveries were adopted for the downstream processing units. The 3-HP recoveries for cell removal, activated-carbon treatment, cation exchange and anion exchange were set to 100.0%, 90.4%, 93.2% and 92.7%, respectively, corresponding to an overall 3-HP recovery of approximately 78.1%. The purified 3-HP stream was subsequently concentrated to the specified final product concentration by evaporation[1].

④Tail Gas treatment and utilities (A400–A500). The off-gas treatment and utility system was integrated into the overall process to recover unreacted gaseous components from the ethanol production section and to utilize combustible by-products for energy recovery. The tail-gas stream leaving the ethanol production unit was first compressed and subsequently introduced into a pressure swing adsorption (PSA) unit for gas separation. Recovered H_2 and CO_2 were recycled to the ethanol production section, thereby reducing the demand for fresh reactants and improving overall carbon utilization. The remaining combustible tail gas was directed to the combined heat and power (CHP) unit for energy recovery and utility generation.

In parallel, the biomass separated from the 3-HP fermentation broth during downstream processing was recovered as a co-product. The wet biomass stream was sent to a spray-drying unit to remove moisture and obtain dry single-cell protein (SCP). The recovered SCP was

considered as a valorized biomass co-product in the overall process model.

Techno-economic analysis. Techno-economic analysis (TEA) was performed to evaluate the economic feasibility of the integrated CO_2-to-3-HP production process. Capital expenditure (CAPEX), operating expenditure (OPEX), and the minimum selling price (MSP) of 3-HP were estimated based on the process simulation results and economic assumptions. The overall process was simulated using Aspen Plus, from which detailed mass and energy balances were obtained for CO_2 hydrogenation and ethanol production (A100), microbial 3-HP production (A200), downstream 3-HP purification (A300), and tail-gas treatment, recycle, and utility generation (A400–A500). Aspen Plus has similarly been used for process-scale TEA of integrated CO_2-derived biomanufacturing systems.

The inside battery limit (ISBL) was defined to include the major process equipment and associated installation costs within the ethanol production, 3-HP production, 3-HP purification, and tail-gas treatment sections. Outside battery limit (OSBL) costs, including utilities, storage, site development, and other supporting facilities, were estimated separately. Economic assumptions and the overall TEA framework were established following published biorefinery techno-economic studies[2-6]. Equipment costs were estimated using conventional capacity-scaling relationships and updated to the selected cost year using the Chemical Engineering Plant Cost Index (CEPCI)[4,7](Supplementary Table 13-15). The MSP of 3-HP was determined as the product selling price at which the net present value (NPV) of the project reached zero at the specified internal rate of return (IRR). Potential credits from co-products and energy recovery, including dry single-cell protein (SCP) and combustible tail-gas utilization, were incorporated where applicable.

Life cycle assessment. Life cycle assessment (LCA) was conducted to evaluate the environmental performance of the integrated CO_2-to-3-HP production process. A cradle-to-gate system boundary was adopted, covering the major process stages from raw-material and energy inputs to the production of 3-HP at the plant gate. The assessed system included CO_2 hydrogenation and ethanol production, microbial 3-HP production, downstream purification, tail-gas treatment and gas recycling, utility generation, and recovery of dry single-cell protein (SCP) from the separated biomass.

The life cycle inventory was established based on the material and energy balances obtained from the Aspen Plus simulation. The inventory included the consumption of CO_2, externally supplied low-carbon H_2, fermentation media, water, process chemicals, electricity, and thermal energy, together with direct process emissions, recycled gas streams, and co-product generation. All externally supplied electricity used in the process was assumed to be generated from solar photovoltaic power.

In the process simulation, the final 3-HP product stream was specified as a 30% (w/v)

aqueous 3-HP solution, consistent with the downstream recovery scheme adopted from the reported 3-HP purification process. For life cycle impact assessment, however, environmental burdens were normalized to the actual mass of 3-HP contained in the product stream. Accordingly, the functional unit was defined as 1 kg of pure 3-HP equivalent at the plant gate.

The global warming potential (GWP) was calculated on the basis of greenhouse-gas emissions associated with raw-material supply, energy consumption, process emissions, and utility requirements across the integrated production system, and was reported as kg CO_2-eq per kg pure 3-HP equivalent (Supplementary Table 16). Internal CO_2 recycle streams were treated as internal process flows rather than additional external inputs. Dry SCP recovered from fermentation biomass was considered a co-product, and its environmental contribution was accounted for using the selected co-product treatment approach. Energy recovered from combustible tail gas in the combined heat and power unit was credited against the corresponding utility demand where applicable.

Supplementary Table S1. Strains used in this study

Strain	Parent Strain	Genotype and plasmid	Source
DH5α	*Escherichia coli*	GenBank: JRYM01000000	Tsingke Biotechnology Co., Ltd.
BL21(DE3)	*E. coli*	GenBank: CP001509.3	Tsingke Biotechnology Co., Ltd.
GS115	*Komagataella phaffii*	*AOX1, his4-*	ATCC® MYA-5012
PO1f	*Yarrowia lipolytica*	*MATα ura3-302 leu2-270 xpr2-322 axp2-ΔNU49 XPR2::SUC2*	ATCC® MYA-2613
NP11	*Rhodotorula toruloides*	GeneBank: GCA_000320785.2	Wuhan Huizao Biotechnology Co., Ltd
BY4741	*Saccharomyces cerevisiae*	*MATα his3Δ1 leu2Δ0 met15Δ0 ura3Δ0*	ATCC® 201388
NCYC495	*Ogataea polymorpha*	GeneBank: GCA_001664045.1	ATCC® 14754
CEN.PK2-1C	*Saccharomyces cerevisiae*	*MATα trp1-289 leu2-3 leu2-112 ura3-52 his3Δ1*	ATCC® MYA-1108
GS115-Cas9	GS115	*His4::*GAPp-Cas9-AOX1t	This study
LT-01	GS115-Cas9	ΔADH2	This study
LT-02	GS115-Cas9	ΔADH6	This study
LT-03	GS115-Cas9	ΔADH7	This study
LT-04	GS115-Cas9	ΔADH900	This study
LT-05	GS115-Cas9	ΔALD1	This study
LT-06	GS115-Cas9	ΔACS1	This study
LT-07	GS115-Cas9	ΔACS2	This study
LT-08	GS115-Cas9	*Int32::*ACS1p-MCR-N-DUS4t, *Int59::*ALD1p-MCR-C-0547t	This study
LT-09	GS115-Cas9	*Int32::*ACS1p-MCR-N-DUS4t, *Int59::*ADH2p-MCR-C-0547t	This study
LT-10	GS115-Cas9	*Int32::*ADH2p-MCR-N-DUS4t, *Int59::*ALD1p-MCR-C-0547t	This study
LT-11	GS115-Cas9	*Int32::*ADH2p-MCR-N-DUS4t, *Int59::*ADH2p-	This study

		MCR-C-0547t	
LT-12	GS115-Cas9	*Int32::*GAPp-MCR-N-DUS4t, *Int59::*ALD1p-MCR-C-0547t	This study
LT-13	GS115-Cas9	*Int32::*GAPp-MCR-N-DUS4t, *Int59::*ADH2p-MCR-C-0547t	This study
LT-14	LT-13	*Int1::*TEF1p-ADH2-FBPt	This study
LT-15	LT-14	*Int10::*GAPp-ADL1-0547t	This study
LT-16	LT-15	*Int11::*ADH2p-ACS1-PMP20t	This study
LT-17	LT-15	*Int11::*GCW14p-ACS1-PMP20t	This study
LT-18	LT-15	*Int11::*TEF1p-ACS1-PMP20t	This study
LT-19	LT-13	HHP-ADH2p-ACS1(wt)-DUS4t	This study
LT-20	LT-13	HHP-ADH2p-ACS1(mutant)-DUS4t	This study
LT-21	LT-13	HHP-ADH2p-ACS1(I658P)-DUS4t	This study
LT-23	BL21(DE3)	pET-28a-ACS1(wt)	This study
LT-24	BL21(DE3)	pET-28a-ACS1(I658P)	This study
LT-25	LT-15	*Int11::*ADH2p-ACS1(I658P)-PMP20t	This study
LT-26	LT-25	*Int31::*TEF1p-ACC1(S1132A)-DUS4t	This study
LT-27	LT-26	*Int21::*GAPp-POS5-DUS4t	This study
LT-28	LT-27	*Int56::*ALD1p-MCR-C-0547t, *Int57::*ADH2p-MCR-N-DUS4t	This study
LT-29	LT-13	HHP-ADH2p-ACS_{SE}(L641P)-DUS4t	This study
LT-30	LT-13	HHP-Promoters-eGFP-DUS4t	This study

Supplementary Table S2. Plasmids used in this study

Plasmids	Description	Source
HHP-sgRNA-His4	gRNAs for targeted gene knock-in or knock-out at specific sites	This study
HHP-sgRNA-ADH2		This study
HHP-sgRNA-ADH6		This study
HHP-sgRNA-ADH7		This study
HHP-sgRNA-ADH900		This study
HHP-sgRNA-ALD1		This study
HHP-sgRNA-ACS1		This study
HHP-sgRNA-ACS2		This study
HHP-sgRNA-Int32		This study
HHP-sgRNA-Int59		This study
HHP-sgRNA-Int1		This study
HHP-sgRNA-Int10		This study
HHP-sgRNA-Int11		This study
HHP-sgRNA-Int31		This study
HHP-sgRNA-Int21		This study
HHP-sgRNA-Int56		This study
HHP-sgRNA-Int57		This study
pPIC9K-His-GAPp-Cas9-AOX1t	For Cas9 integration	This study
HZP-Int32-Donor	Donor helper plasmids containing upstream and downstream homology arms	This study
HZP-Int59-Donor		This study
HZP-Int1-Donor		This study
HZP-Int10-Donor		This study
HZP-Int11-Donor		This study
HZP-Int31-Donor		This study
HZP-Int21-Donor		This study
HZP-Int56-Donor		This study
HZP-Int57-Donor		This study
HZP-Int32-ACS1p-MCR-N-DUS4t	Donor plasmids for targeted gene knock-in at specific sites	This study
HZP-Int32-ADH2p-MCR-N-DUS4t		This study
HZP-Int32-GAPp-MCR-N-DUS4t		This study
HZP-Int59-ALD1p-MCR-C-0547t		This study
HZP-Int59-ADH2p-MCR-C-0547t		This study
HZP-Int1-TEF1p-ADH2-FBPt		This study
HZP-Int10-GAPp-ALD1-0547t		This study

HZP-Int11-ADH2p-ACS1-PMP20t		This study
HZP-Int11-GCW14p-ACS1-PMP20t		This study
HZP-Int11-TEF1p-ACS1-PMP20t		This study
HZP-Int11-ADH2p-ACS1(I658P)-PMP20t		This study
HZP-Int31-TEF1p-ACC1(S1132A)-DUS4t		This study
HZP-Int21-GAPp-POS5-DUS4t		This study
HZP-Int56-ALD1p-MCR-C-0547t		This study
HZP-Int57-ADH2p-MCR-N-DUS4t		This study
HHP-ADH2p-ACS_{SE}(L641P)-DUS4t	Plasmid for expression of single-site mutant of *S. enterica* ACS in yeast	This study
HHP-ADH2p-ACS1(wt)-DUS4t	Plasmid for expression of wild type of *K. phaffii* ACS1 in yeast	This study
HHP-ADH2p-ACS1(N557P)-DUS4t	Plasmids for expression of single-site mutants of *K. phaffii* ACS1 in yeast	This study
HHP-ADH2p-ACS1(Y498H)-DUS4t		This study
HHP-ADH2p-ACS1(S274L)-DUS4t		This study
HHP-ADH2p-ACS1(A520R)-DUS4t		This study
HHP-ADH2p-ACS1(G320A)-DUS4t		This study
HHP-ADH2p-ACS1(P25K)-DUS4t		This study
HHP-ADH2p-ACS1(L301A)-DUS4t		This study
HHP-ADH2p-ACS1(N12K)-DUS4t		This study
HHP-ADH2p-ACS1(R70L)-DUS4t		This study
HHP-ADH2p-ACS1(R70V)-DUS4t		This study
HHP-ADH2p-ACS1(I14F)-DUS4t		This study
HHP-ADH2p-ACS1(S574Q)-		This study

DUS4t		
HHP-ADH2p-ACS1(I14Y)-DUS4t		This study
HHP-ADH2p-ACS1(A520K)-DUS4t		This study
HHP-ADH2p-ACS1(Q138N)-DUS4t		This study
HHP-ADH2p-ACS1(V371T)-DUS4t		This study
HHP-ADH2p-ACS1(R70I)-DUS4t		This study
HHP-ADH2p-ACS1(G312E)-DUS4t		This study
HHP-ADH2p-ACS1(F52W)-DUS4t		This study
HHP-ADH2p-ACS1(N12R)-DUS4t		This study
HHP-ADH2p-ACS1(G281A)-DUS4t		This study
HHP-ADH2p-ACS1(G402A)-DUS4t		This study
HHP-ADH2p-ACS1(I627A)-DUS4t		This study
HHP-ADH2p-ACS1(K626A)-DUS4t		This study
HHP-ADH2p-ACS1(M628A)-DUS4t		This study
HHP-ADH2p-ACS1(Q430A)-DUS4t		This study
HHP-ADH2p-ACS1(D517A)-DUS4t		This study
HHP-ADH2p-ACS1(K210A)-DUS4t		This study
HHP-ADH2p-ACS1(R532A)-DUS4t		This study
HHP-ADH2p-ACS1(T427A)-DUS4t		This study
HHP-ADH2p-ACS1(Y428A)-DUS4t		This study
HHP-ADH2p-ACS1(F179A)-DUS4t		This study
HHP-ADH2p-ACS1(R207A)-DUS4t		This study

HHP-ADH2p-ACS1(R623A)-DUS4t		This study
HHP-ADH2p-ACS1(S650A)-DUS4t		This study
HHP-ADH2p-ACS1(T348A)-DUS4t		This study
HHP-ADH2p-ACS1(T648A)-DUS4t		This study
HHP-ADH2p-ACS1(S280A)-DUS4t		This study
HHP-ADH2p-ACS1(T622A)-DUS4t		This study
HHP-ADH2p-ACS1(R630A)-DUS4t		This study
HHP-ADH2p-ACS1(D426A)-DUS4t		This study
HHP-ADH2p-ACS1(Y428F)-DUS4t		This study
HHP-ADH2p-ACS1(D534A)-DUS4t		This study
HHP-ADH2p-ACS1(D534N)-DUS4t		This study
HHP-ADH2p-ACS1(D534S)-DUS4t		This study
HHP-ADH2p-ACS1(E432Q)-DUS4t		This study
HHP-ADH2p-ACS1(F179Y)-DUS4t		This study
HHP-ADH2p-ACS1(F182Y)-DUS4t		This study
HHP-ADH2p-ACS1(K626R)-DUS4t		This study
HHP-ADH2p-ACS1(R543K)-DUS4t		This study
HHP-ADH2p-ACS1(W324F)-DUS4t		This study
HHP-ADH2p-ACS1(I658P)-DUS4t		This study
HHP-ADH2p-ACS1(I658P+A520K)-DUS4t	Plasmids for expression of multi-site mutants of *K. phaffii* ACS1 in yeast	This study
HHP-ADH2p-ACS1(I658P+A520R)-DUS4t		This study
HHP-ADH2p-ACS1(I658P+K626A)-DUS4t		This study

HHP-ADH2p-ACS1(I658P+N557P)-DUS4t		This study
HHP-ADH2p-ACS1(I658P+R543K)-DUS4t		This study
HHP-ADH2p-ACS1(I658P+T348A)-DUS4t		This study
HHP-ADH2p-ACS1(I658P+W324F)-DUS4t		This study
HHP-ADH2p-ACS1(I658P+Y428F)-DUS4t		This study
pET-28a-ACS1(wt)	Plasmids for recombinant expression of wild-type and mutant ACS1 proteins in *E. coli* BL21(DE3)	This study
pET-28a-ACS1(I658P)		This study
HHP-AOX1p-eGFP-DUS4t	Plasmids for reporter assay of 22 endogenous promoters fused to eGFP in *K. phaffii*	This study
HHP-AOX2*p-eGFP-DUS4t		This study
HHP-GAPp-eGFP-DUS4t		This study
HHP-CDC19p-eGFP-DUS4t		This study
HHP-TEF1p-eGFP-DUS4t		This study
HHP-PDC1p-eGFP-DUS4t		This study
HHP-ADH2p-eGFP-DUS4t		This study
HHP-ADH6p-eGFP-DUS4t		This study
HHP-ADH7p-eGFP-DUS4t		This study
HHP-ADH900p-eGFP-DUS4t		This study
HHP-ICL1p-eGFP-DUS4t		This study
HHP-ACS1p-eGFP-DUS4t		This study
HHP-ALD1p-eGFP-DUS4t		This study
HHP-DOG1p-eGFP-DUS4t		This study
HHP-DAS1p-eGFP-DUS4t		This study
HHP-DAS2p-eGFP-DUS4t		This study
HHP-PMP20p-eGFP-DUS4t		This study
HHP-FDHp-eGFP-DUS4t		This study
HHP-FLD1p-eGFP-DUS4t		This study
HHP-GCW14p-eGFP-DUS4t		This study
HHP-CAT1p-eGFP-DUS4t		This study
HHP-LAR3p-eGFP-DUS4t		This study

Supplementary Table S3. Main primers used in this study

Primer	Sequence (5′-3′)	Description
AOX1-F	CACGAGGgatctaacatccaaagacgaaag	Primers for amplification of promoter sequences from the GS115 genome. Note: The AOX2* promoter contains a T to C mutation at position −255.
AOX1-R	TAGAAACCATttcgaataattagttgttttttgatcttc	
AOX2*-F	ATCACGAGGTTTTTTTCAGACCATATGACCG	
AOX2*-R	CTTTAGAAACCATTTTTTCTCAGTTGATTTGTTTGT	
GAP-F	TATCACGAGGCTGCTACTCTGGTCCCAAG	
GAP-R	AGAAACCATTGTGTTTTGATAGTTGTTCAATTGAT	
CDC19-F	TATCACGAGGTTCAGTGTGCGGGATACTGTA	
CDC19-R	CTTTAGAAACCATTGGATTGATTTCAGTTAAAAAAAAGTCTAAA	
TEF1-F	ACGAGGGGTAATAACTGTCGCCTCTTT	
TEF1-R	TTAGAAACCATGTTGGCGAATAACTAAAATG	
PDC1-F	CGAGGGGGACAAGCACACGATTAC	
PDC1-R	GAAACCATTGTTGTGTACTAGCTAATTGATTG	
ADH2-F	TATCACGAGGCGATTGCCCCTCTACAGGCATAAG	
ADH2-R	CCTTTAGAAACCATTTTCGTAAAGTAAATAAGATAAAAGCTAGTAG	
ADH6-F	GTATCACGAGGCTTGGGGAACACAGTTGAAAG	
ADH6-R	AGAAACCATTGTTTGGTTTTTACTAGTTTTCT	
ADH7-F	CGTATCACGAGGTCAAAAATTCACGGTAGAAACTGAAG	
ADH7-R	CCTTTAGAAACCATTTGTTATAGTGATGAAATAAAAAATTAAAAATAAG	
ADH900-F	GTATCACGAGGTCCAGTTGGGCCATTACCGA	
ADH900-R	TAGAAACCATTGGTTATGGGGAATTGACTATCT	
ICL1-F	CACGAGGTAACACTTTGTATAGCACATCGTAC	
ICL1-R	CCTTTAGAAACCATTCTTGATATACTTGATACTGTGTTCTTT	
ACS1-F	TCACGAGGTAAAACCACCAGCTAGTACAGAG	
ACS1-R	CACCTTTAGAAACCATAATTGATCAACAACTAAGTCGTATC	
ALD1-F	TATCACGAGGAGACCAGCAGTTTAACTACG	
ALD1-R	AAACCATCTTTTCTTTGGGCAAGGAAAA	
DOG1-F	TCACGAGGGAACCGTGGTAAATGACGAATG	
DOG1-R	GAAACCATTATTGTTTGTTGATGGTTTTCAC	
DAS1-F	ATCACGAGGCTATGCTACCCCACAGAAATACC	
DAS1-R	TTAGAAACCATTTTTGATGTTTGATAGTTTGATAAGAGT	
DAS2-F	CACGAGGAGCAATGATATAAACAACAATTGAGT	
DAS2-R	TTTAGAAACCATTTTGTTCGATTATTCTCCAGATAAAA	
PMP20-F	TATCACGAGGTTCTGGAGTGTCAAAACAGTAGTGA	
PMP20-R	CCTTTAGAAACCATCTTAGAATTTTTTTTTTTGTCTTGGTGGGA	
FDH-F	TATCACGAGGTGGGTGCGGAACCAGCTTCTA	
FDH-R	TAGAAACCATTGTTTAAGTGGGTGATGTTGGAGGT	
FLD1-F	TATCACGAGGTGCAGGAATCTCTGGCACG	
FLD1-R	TTAGAAACCATTGTGAATATCAAGAATTGTATGAACAAGCAAAG	
GCW14-F	ATCACGAGGCAGGTGAACCCACCTAACTATTTT	

GCW14-R	TTTAGAAACCATTTTTGTTGTTGAGTGAAGCGAGT	
CAT1-F	TATCACGAGGCTATGTTGACGGAGAGTGTTG	
CAT1-R	TTAGAAACCATTTTAATTGTAAGTCTTGACTAGAGCAA	
LAR3-F	CACGAGGTTAAACTGAAAGAACAAAGAACCAGT	
LAR3-R	TTTAGAAACCATATTTTTAGGAGATAAAAATTCTGGGGTA	
Int59-donor-F	TATCACGAGGTTGGCACCAAAAGAGTAACC	Primers for construction of the donor helper plasmid (HZP-Int59-Donor)
Int59-donor-R	ggagctcGTCCAAGTCTCTCACGATGGTG	
59-BB-F	AGAGACTTGGACgagctccctgcaggcat	
59-BB-R	TTTTGGTGCCAACCTCGTGATACGCCTATTTTTATAGGTTAAT	
Int32-donor-F	TATCACGAGGGTGTCGAACATGGTTGGGAACCT	Primers for construction of the donor helper plasmid (HZP-Int32-Donor)
Int32-donor-R	ctgcagggagctcCAGCTACTGATTTTGGAGCACC	
32-BB-F	CAGTAGCTGgagctccctgcaggcatgc	
32-BB-R	CATGTTCGACACCCTCGTGATACGCCTATTTTTATAGG	
Int1-donor-F	TATCACGAGGACCTTTCGCTTTTGAACATTCTAAC	Primers for construction of the donor helper plasmid (HZP-Int1-Donor)
Int1-donor-R	gcagggagctcGGACTACGTGGCTCTCAAGTT	
1-BB-F	CCACGTAGTCCgagctccctgcaggcatg	
1-BB-R	AAAAGCGAAAGGTCCTCGTGATACGCCTATTTTTATAGGT	
Int10-donor-F	TATCACGAGGGCCACAGTCACAATTCTTTACTCC	Primers for construction of the donor helper plasmid (HZP-Int10-Donor)
Int10-donor-R	gcagggagctcCACAACAACAACAACAACTATTCAAAACA	
10-BB-F	TGTTGTTGTGgagctccctgcaggcat	
10-BB-R	TTGTGACTGTGGCCCTCGTGATACGCCTATTTTTATAGGT	
Int11-donor-F	TATCACGAGGCGAATAGACGCGTATTCGCAG	Primers for construction of the donor helper plasmid (HZP-Int11-Donor)
Int11-donor-R	ctgcagggagctcATTTTCTTAAATACTGGCGCGTCC	
11-BB-F	TAAGAAAATgagctccctgcaggcatg	
11-BB-R	CGCGTCTATTCGCCTCGTGATACGCCTATTTTTATAGGT	
Int21-donor-F	TATCACGAGGATTATCCAGGGTGCTTGGTCG	Primers for construction of the donor helper plasmid (HZP-Int21-Donor)
Int21-donor-R	cagggagctcGGGTGCTACATTTTGTTTCAGGAAGG	
21-BB-F	GTAGCACCCgagctccctgcaggcatg	
21-BB-R	CCTGGATAATCCTCGTGATACGCCTATTTTTATAGGTTAAT	
Int31-donor-F	TATCACGAGGCCCAGATTTTCAACTTTGTTTACTCC	Primers for construction of the donor
Int31-donor-R	cagggagctcGCCCTTTGTGAAATCACATGAC	
31-BB-F	TTCACAAAGGGCgagctccctgcaggcatg	

31-BB-R	GAAAATCTGGGCCTCGTGATACGCCTATTTTTATAGGT	helper plasmid (HZP-Int31-Donor)
Int56-donor-F	TATCACGAGGCAATTGAATATTTGGACTGTTTCTCAT	Primers for construction of the donor helper plasmid (HZP-Int56-Donor)
Int56-donor-R	cagggagctcATCAGCTTCATCAATTTCTTCCAAT	
56-BB-F	TGATGAAGCTGATgagctccctgcaggcatg	
56-BB-R	ATATTCAATTGCCTCGTGATACGCCTATTTTTATAGGT	
Int57-donor-F	TATCACGAGGAATCCTTGGTAATCAGAAGAAACATCA	Primers for construction of the donor helper plasmid (HZP-Int57-Donor)
Int57-donor-R	agggagctcTGGTACTCAATTAAAAGGATACACCTAA	
57-BB-F	TAATTGAGTACCAgagctccctgcaggcatg	
57-BB-R	TACCAAGGATTCCTCGTGATACGCCTATTTTTATAGGT	
BB-F-mutant	AGGACTATAAAGATACCAGGCGTTTCC	Primers for construction of 20 AI-predicted ACS1 mutants
BB-R-mutant	CCTGGTATCTTTATAGTCCTGTCGGGTTTC	
G320A-F	TTTATTCACTGCTGCTGATGTGGGCTGGATCACAGGG	
G320A-R	CCCACATCAGCAGCAGTGAATAAAATATCATCACCCTGAAC	
L301A-F	GGAGCTGCTTTGACCACCAAGTATGTCTTTGATGTTCAG	
L301A-R	CTTGGTGGTCAAAGCAGCTCCCAGTAAGTAGCCAGC	
N12K-F	CTTACTTCATGAAAAGTCCATTGACCCACCAAAGGGATTC	
N12K-R	GGACTTTTCATGAAGTAAGTGTTCGTTATCTAATGGCA	
N557P-F	CTAATCGAACACCCATTGGTAGGAGAGTCTGCTGTCG	
N557P-R	TACCAATGGGTGTTCGATTAGAGCGCTTTCAATCTC	
P25K-F	AAAGACACAAGGGAACTCCTAATATACCAGGCGGTTG	
P25K-R	AGGAGTTCCCTTGTGTCTTTCAAAGAATCCCTTTGGTGG	
S274L-F	TGAAGATACTCTGTTTTTGCTTTACACTTCTGGCTCTACCG	
S274L-R	GCAAAAACAGAGTATCTTCAGATCTAACATTCACTGGGG	
Y498H-F	TCTGGAAGGACCACAACCGTTTCCTGGATACATATCTCAGG	
Y498H-R	ACGGTTGTGGTCCTTCCAGACTGTTCTAGCCATAGA	
A520R-F	TGATGGAGCTCGTAGAGATCAGGAAGGATTTTATTGGGTTCT	
A520R-R	GATCTCTACGAGCTCCATCACCAGTGAAGTAATAACC	
A520K-F	GATGGAGCTAAGAGAGATCAGGAAGGATTTTATTGGGTTCT	
A520K-R	CTGATCTCTCTTAGCTCCATCACCAGTGAAGTAATAACC	
F52W-F	CAAAGTTTTGGGGAGAAAAAGCAAAGGAATTCTTGTCATGG	
F52W-R	TTTTTCTCCCCAAAACTTTGAGGGGTTCTCGATGG	
G312E-F	TGTTCAGGAAGATGATATTTTATTCACTGCTGGTGATGTGG	
G312E-R	AAATATCATCTTCCTGAACATCAAAGACATACTTGGTGGTCA	
I14F-F	CATGAAAATTCCTTTGACCCACCAAAGGGATTCTTTGAAA	
I14F-R	GGTCAAAGGAATTTTCATGAAGTAAGTGTTCGTTATCTAATGG	
I14Y-F	TGAAAATTCCTACGACCCACCAAAGGGATTCTTTGAAAG	
I14Y-R	TGGGTCGTAGGAATTTTCATGAAGTAAGTGTTCGTTATCTAAT	

N12R-F	TACTTCATGAACGTTCCATTGACCCACCAAAGGGATTC	
N12R-R	TCAATGGAACGTTCATGAAGTAAGTGTTCGTTATCTAATGGCA	
Q138N-F	GCCAACGTATTGACTGACCTGGGTGTGAAAAA	
Q138N-R	AGGTCAGTCAATACGTTGGCAATTCGACAAACATCCTTCAG	
R70I-F	TTCACTGACGCTATTTACCCACCTGGTAATGGATTTCAGAAT	
R70I-R	AGGTGGGTAAATAGCGTCAGTGAAAGGAGTAGCC	
R70L-F	ACTGACGCTCTGTACCCACCTGGTAATGGATTTCAGAATG	
R70L-R	ACCAGGTGGGTACAGAGCGTCAGTGAAAGGAGTAGC	
R70V-F	TGACGCTGTTTACCCACCTGGTAATGGATTTCAGAAT	
R70V-R	CCAGGTGGGTAAACAGCGTCAGTGAAAGGAGTAGC	
S574Q-F	TGACTGGTCAAGCTGTGGCCGCGTTTGTGTCTTT	
S574Q-R	CCACAGCTTGACCAGTCAGCTCGTCAGGG	
V371T-F	TACTCAGTTTTATACTGCACCAACTGCTCTTAGGTTGC	
V371T-R	TGGTGCAGTATAAAACTGAGTAACTTTGTGTTTGTCAACG	
BB-F-mutant	AGGACTATAAAGATACCAGGCGTTTCC	Primers for construction of 32 semi-rationally designed ACS1 mutants
BB-R-mutant	CCTGGTATCTTTATAGTCCTGTCGGGTTTC	
G281A-F	TGCTTTACACTTCTGCTTCTACCGGAAAGCCTAAAGGTATCC	
G281A-R	GGTAGAAGCAGAAGTGTAAAGCAAAAATGAAGTATCTTCAGATCT	
G402A-F	TTTTGGGTTCCGTTGCTGAACCTATAGCCGCTGAAGTTTGG	
G402A-R	ATAGGTTCAGCAACGGAACCCAAAACCCTGATTGAA	
I627A-F	AGATCAGGTAAGGCTATGAGACGTATTCTCAGAAAGGTTTTGGC	
I627A-R	AATACGTCTCATAGCCTTACCTGATCTGGTCTTTGGAAGATCAC	
K626A-F	TCAGGTGCTATAATGAGACGTATTCTCAGAAAGGTTTTGG	
K626A-R	TACGTCTCATTATAGCACCTGATCTGGTCTTTGGAAGATCAC	
M628A-F	AGGTAAGATAGCTAGACGTATTCTCAGAAAGGTTTTGGCT	
M628A-R	ATACGTCTAGCTATCTTACCTGATCTGGTCTTTGGAAGATCAC	
Q430A-F	TACGTATTGGGCTACAGAGACTGGTTCTCACATTATTGCT	
Q430A-R	CAGTCTCTGTAGCCCAATACGTATCACAAATATGAGCTTTTCCT	
R630A-F	GATAATGAGAGCTATTCTCAGAAAGGTTTTGGCTGGAGA	
R630A-R	TTCTGAGAATAGCTCTCATTATCTTACCTGATCTGGTCTTTGG	
S280A-F	TGCTTTACACTGCTGGCTCTACCGGAAAGCCTAAAGG	
S280A-R	AGAGCCAGCAGTGTAAAGCAAAAATGAAGTATCTTCAGATCTAAC	
T622A-F	ATCTTCCAAAGGCTAGATCAGGTAAGATAATGAGACGTATTCTCAGA	
T622A-R	TTACCTGATCTAGCCTTTGGAAGATCACTTACCAAGATGATGAGT	
T648A-F	GGCGACATTTCAGCTCTTTCAAACCCTTCGATTGTGGAAGAG	
T648A-R	GGTTTGAAAGAGCTGAAATGTCGCCCAGAGAGTCTTC	
D517A-F	TACTTCACTGGTGCTGGAGCTGCCAGAGATCAGGA	
D517A-R	GCAGCTCCAGCACCAGTGAAGTAATAACCTTCATATGGCC	
K210A-F	TGAGAGGTGGGGCTATCATCGAGACTAAGAAGATTGTTGACGAG	
K210A-R	CTCGATGATAGCCCCACCTCTCAGAGATTCATCAGAAG	
R532A-F	TTGGGTTCTGGGTGCTGTTGATGATGTTGTTAATGTGTCAGGTCAC	
R532A-R	ATCAACAGCACCCAGAACCCAATAAAATCCTTCCT	
T427A-F	CTCATATTTGTGATGCTTATTGGCAAACAGAGACTGGTTCTCAC	

T427A-R	TGCCAATAAGCATCACAAATATGAGCTTTTCCTCTTCCAAC	
Y428A-F	TTTGTGATACGGCTTGGCAAACAGAGACTGGTTCTCAC	
Y428A-R	CTGTTTGCCAAGCCGTATCACAAATATGAGCTTTTCCTCTTCC	
F179A-F	ATCCACTCTGTTGTCGCTGCAGGTTTTTCAGCTGGTTCTCT	
F179A-R	CCTGCAGCGACAACAGAGTGGATAGCACCGATTCTA	
R207A-F	TGATGAATCTCTGGCTGGTGGGAAGATCATCGAGACTAAGAA	
R207A-R	CACCAGCCAGAGATTCATCAGAAGTGATAACAATTCTAGAATCAG	
R623A-F	CAAAGACCGCTTCAGGTAAGATAATGAGACGTATTCTCAGAAAGG	
R623A-R	ATCTTACCTGAAGCGGTCTTTGGAAGATCACTTACCAAGATG	
S650A-F	CATTTCAACTCTTGCTAACCCTTCGATTGTGGAAGAGATAATCT	
S650A-R	CGAAGGGTTAGCAAGAGTTGAAATGTCGCCCAGAGAG	
T348A-F	TTGTTTTTGAGGGCGCTCCAGCTTACCCAGACTATTCACGT	
T348A-R	GCTGGAGCGCCCTCAAAAACAACTGTCGTAGC	
I658P-F	ATTGTGGAAGAGCCAATCTCTACCGTTAAAAGGGATG	
I658P-R	AACGGTAGAGATTGGCTCTTCCACAATCGAAGGGTTT	
D426N-F	GCTCATATTTGTAACACGTATTGGCAAACAGAGACTGG	
D426N-R	ATACGTGTTACAAATATGAGCTTTTCCTCTTCCAACATACT	
D534A-F	GGGTAGAGTTGCTGATGTTGTTAATGTGTCAGGTCACAGAT	
D534A-R	AACATCAGCAACTCTACCCAGAACCCAATAAAATCCTT	
D534N-F	TGGGTAGAGTTAACGATGTTGTTAATGTGTCAGGTCACAGATT	
D534N-R	CAACATCGTTAACTCTACCCAGAACCCAATAAAATCCTTC	
D534S-F	GTAGAGTTAGTGATGTTGTTAATGTGTCAGGTCACAGAT	
D534S-R	TAACAACATCACTAACTCTACCCAGAACCCAATAAAATCCTTC	
E432Q-F	GGCAAACACAAACTGGTTCTCACATTATTGCTCCAAT	
E432Q-R	GAACCAGTTTGTGTTTGCCAATACGTATCACAAATATGAGCT	
F179Y-F	CACTCTGTTGTCTACGCAGGTTTTTCAGCTGGTTCTCT	
F179Y-R	AAAACCTGCGTAGACAACAGAGTGGATAGCACCG	
F182Y-F	TTGTCTTCGCAGGTTACTCAGCTGGTTCTCTACGTGATCG	
F182Y-R	AGCTGAGTAACCTGCGAAGACAACAGAGTG	
K626R-F	ATCAGGTCGTATAATGAGACGTATTCTCAGAAAGGTTTTGG	
K626R-R	GTCTCATTATACGACCTGATCTGGTCTTTGGAAGATCAC	
R543K-F	TCAGGTCACAAGTTGTCTACTGCCGAGATTGAAAGC	
R543K-R	GTAGACAACTTGTGACCTGACACATTAACAACATCATCA	
W324F-F	TGATGTGGGCTTCATCACAGGGCATTCTTATGTAGTTTACGG	
W324F-R	CTGTGATGAAGCCCACATCACCAGCAGTGAATA	
Y428F-F	TTGTGATACGTTCTGGCAAACAGAGACTGGTTCTCAC	
Y428F-R	TTTGCCAGAACGTATCACAAATATGAGCTTTTCCTCTTCC	

Supplementary Table S4. Genes overexpressed or knocked out in this study

Gene	Source	Modification	NCBI Accession No.
ADH2	*K. phaffii* GS115	no	XM_002491337.1
ADH6	*K. phaffii* GS115	no	XM_002493969.1
ADH7	*K. phaffii* GS115	no	XM_002489969.1
ADH900	*K. phaffii* GS115	no	XM_002491163.1
ALD1	*K. phaffii* GS115	no	XM_002491373.1
ACS1	*K. phaffii* GS115	no	XP_002491701.1
ACS2	*K. phaffii* GS115	no	XM_002492586.1
MCR-N	*C. aurantiacus*	Codon optimized for yeast	AY530019.1
MCR-C (N940V/K1106W/S1114R)	*C. aurantiacus*	Codon optimized for yeast and carrying the N940V/K1106W/S1114R mutations	AY530019.1
ACS_{SE}(L641P)	*S. enterica*	Codon optimized for yeast and carrying the L641P mutation	AAL23099.1
ACC1(S1132A)	*K. phaffii* GS115	S1132A mutation	XP_002490365.1
POS5	*S. cerevisiae*	Codon optimized for *K. phaffii* and lacking the N-terminal 17 amino acids	NP_015136.1

Supplementary Table S5. Synthesized genes used in this study

Gene	Sequence (5′-3′)
MCR-N	ATGTCTGGTACAGGTAGATTGGCCGGAAAGATTGCTCTGATT ACTGGTGGTGCTGGTAACATTGGTTCTGAATTGACTAGAAGA TTTTTGGCTGAAGGTGCTACTGTTATTATTTCTGGTAGAAACA GAGCTAAGTTGACTGCTTTAGCTGAAAGAATGCAAGCTGAA GCTGGTGTTCCAGCTAAGAGAATTGATCTGGAAGTTATGGAT GGTTCTGATCCTGTTGCTGTCAGAGCCGGTATTGAAGCTATT GTTGCTAGACATGGTCAAATTGATATTTTGGTTAACAACGCTG GATCTGCCGGTGCCCAAAGAAGATTGGCTGAAATTCCATTGA CTGAAGCTGAACTGGGTCCAGGTGCTGAAGAAACTTTGCAC GCTTCTATTGCTAACTTGCTTGGAATGGGTTGGCATTTGATGA GAATTGCTGCTCCACACATGCCAGTTGGTTCTGCCGTTATTA ACGTTTCTACTATTTTTAGTAGAGCTGAGTACTACGGACGTAT TCCATACGTTACTCCAAAGGCTGCTTTGAATGCTCTTTCTCAA CTTGCTGCTAGAGAATTAGGTGCTAGAGGAATTAGAGTTAAC ACTATTTTTCCTGGTCCAATTGAATCTGATAGAATTAGAACTG TTTTCCAAAGAATGGATCAATTGAAGGGTAGACCTGAAGGT GACACTGCTCATCACTTTTTGAATACTATGAGATTGTGTAGAG CTAACGACCAAGGTGCTCTTGAACGTAGATTTCCTTCTGTTG GAGATGTTGCTGATGCTGCTGTTTTTCTTGCTTCTGCTGAATC TGCTGCTTTAAGTGGTGAAACTATTGAAGTGACTCATGGTAT GGAATTACCAGCTTGTTCAGAAACTTCTTTGTTAGCTAGAAC CGATTTGAGAACTATTGATGCATCTGGTAGAACTACCTTGATT TGTGCTGGTGACCAAATTGAAGAAGTTATGGCTTTGACTGGT ATGTTGAGAACTTGTGGTTCTGAAGTTATTATTGGTTTTAGAT CCGCTGCTGCTTTAGCTCAATTTGAACAAGCTGTTAACGAAT CAAGAAGGTTAGCCGGTGCTGATTTCACTCCACCTATTGCAT TGCCATTAGATCCAAGGGACCCAGCCACTATTGACGCTGTTT TTGATTGGGCTGGTGAAAACACCGGTGGAATCCATGCAGCA GTTATTTTGCCTGCTACCTCTCATGAACCTGCTCCATGTGTCA TTGAAGTTGATGATGAAAGAGTTTTGAACTTTTTGGCTGATG AGATTACTGGAACTATTGTTATTGCTTCCAGATTAGCTAGATA CTGGCAATCTCAAAGGTTGACTCCAGGTGCTAGAGCTAGAG GACCAAGAGTTATCTTTTTGTCTAACGGTGCTGATCAAAACG GAAACGTTTACGGTAGGATTCAATCTGCTGCTATTGGTCAATT GATTAGAGTTTGGAGACATGAAGCTGAATTGGATTACCAAAG AGCTTCTGCTGCTGGAGATCATGTTTTGCCACCAGTTTGGGC TAACCAGATTGTTAGATTTGCTAACAGATCTCTTGAAGGTTTG GAATTTGCTTGTGCTTGGACTGCTCAATTGTTGCATTCTCAA AGACATATTAACGAAATTACTTTGAACATTCCAGCTAACTAA

MCR-C (N940V/K1106W /S1114R)	ATGTCTGCTACCACTGGTGCTAGGTCTGCTTCTGTCGGTTGG GCTGAGTCTTTGATCGGTTTGCACCTTGGAAAAGTCGCCCTT ATCACCGGAGGATCTGCCGGTATTGGTGGTCAGATCGGTAGG CTTTTGGCTTTGAGTGGAGCTAGAGTCATGTTGGCTGCTAGA GATAGACATAAGCTTGAGCAGATGCAAGCCATGATCCAGTCT GAGCTTGCCGAGGTCGGATACACTGACGTCGAGGACAGAGT CCATATTGCCCCCGGTTGCGACGTCAGTAGTGAAGCCCAACT TGCCGACTTGGTCGAAAGGACCCTTTCTGCCTTTGGAACCGT CGACTATTTGATCAACAATGCCGGTATTGCCGGTGTCGAAGA AATGGTCATCGACATGCCAGTCGAGGGATGGAGGCACACCT TGTTTGCCAACTTGATTAGTAATTATTCTTTGATGAGGAAGCT TGCCCCACTTATGAAGAAGCAAGGTTCTGGTTATATTCTTAAT GTCAGTTCTTATTTCGGTGGAGAGAAGGACGCCGCCATTCCA TACCCAAATAGGGCTGACTACGCCGTTAGTAAGGCTGGACA GAGAGCCATGGCTGAAGTCTTTGCTAGATTCTTGGGTCCAGA GATCCAGATCAATGCCATCGCCCCCGGTCCAGTTGAGGGAG ATAGACTTAGGGGAACTGGTGAAAGGCCCGGTCTTTTCGCTA GGAGGGCTAGACTTATCCTTGAGAATAAGAGGCTTAACGAA CTTCACGCCGCTCTTATCGCTGCTGCCAGAACCGATGAGAGG AGTATGCACGAGTTGGTCGAATTGCTTTTGCCAAACGACGTT GCCGCCTTGGAACAGAATCCAGCTGCCCCAACTGCTCTTAG GGAGTTGGCTAGAAGGTTTAGAAGTGAAGGAGATCCAGCCG CCTCTTCTAGTTCTGCTTTGCTTAATAGATCTATCGCCGCCAA GCTTTTGGCCAGACTTCACAACGGTGGATACGTTTTGCCAGC CGACATCTTCGCTAACTTGCCAAACCCACCAGACCCTTTCTT CACCAGAGCCCAAATCGATAGAGAGGCTAGAAAGGTTAGAG ACGGTATCATGGGAATGTTGTACTTGCAGAGGATGCCAACCG AATTTGATGTTGCCATGGCTACCGTTTACTACTTGGCTGATAG GGTCGTCTCTGGTGAAACCTTCCATCCAAGTGGAGGTTTGA GGTACGAGAGGACCCCAACCGGAGGAGAGCTTTTCGGTCTT CCTTCTCCAGAGAGGTTGGCCGAATTGGTCGGTTCTACCGTC TACCTTATTGGAGAGCACTTGACCGAACATTTGAATTTGCTT GCTAGAGCCTACCTTGAAAGGTACGGAGCCAGACAAGTTGT TATGATCGTCGAAACCGAGACTGGAGCTGAGACCATGAGGA GACTTCTTCACGACCACGTTGAGGCTGGAAGATTGATGACC ATCGTCGCTGGAGACCAGATTGAGGCTGCCATCGACCAAGC TATCACTAGATATGGAAGACCCGGTCCAGTTGTCTGTACTCCT TTCAGACCTCTTCCAACCGTCCCTTTGGTCGGTAGGAAGGAT AGTGACTGGTCTACCGTCTTGAGTGAGGCCGAATTCGCCGA ACTTTGCGAACACCAACTTACCCACCATTTCAGAGTCGCTAG ATGGATTGCTCTTAGTGATGGTGCCAGACTTGCTTTGGTCAC TCCAGAAACCACCGCCACCAGTACCACCGAACAGTTCGCCT TGGCCAACTTCATCAAGACTACCTTGCACGCTTTCACCGCCA CTATTGGAGTTGAGTCTGAAAGGACCGCCCAGAGGATCTTG

	ATCAACCAAGTTGACCTTACCAGAAGGGCTAGGGCCGAGGA ACCTAGAGATCCTCACGAAAGGCAGCAAGAACTTGAGAGGT TCATCGAGGCCGTCCTTTTGGTTACTGCTCCTTTGCCTCCAG AAGCCGATACCAGATATGCTGGAAGGATCCATAGAGGAAGA GCTATCACTGTCTAA
ACS_{SE}(L641P)	ATGTCTCAAACTCATAAGCATGCTATTCCAGCTAATATTGCTG ATAGATGTTTGATTAACCCAGAACAATATGAAACTAAGTACA AACAATCCATCAACGATCCAGATACTTTTTGGGGTGAACAAG GTAAGATTTTGGATTGGATTACTCCATATCAAAAGGTTAAAA ACACCTCTTTCGCTCCAGGTAACGTTTCTATTAAGTGGTACG AAGATGGTACTTTGAACTTGGCTGCTAATTGTTTGGATAGAC ATTTGCAAGAAAACGGTGATAGAACTGCTATTATTTGGGAAG GTGATGATACTTCTCAATCTAAACATATTTCCTACAGAGAATT GCATAGAGATGTTTGTAGATTCGCTAATACTTTGTTGGATTTG GGTATTAAGAAGGGTGATGTTGTTGCTATTTACATGCCAATGG TTCCAGAAGCTGCTGTTGCTATGTTGGCTTGTGCTAGAATTG GTGCTGTTCATTCTGTTATTTTTGGTGGTTTTTCTCCTGAAGC TGTTGCTGGTAGAATTATTGATTCTTCTTCTAGATTGGTCATC ACTGCTGATGAAGGTGTTAGAGCTGGTAGATCTATTCCTTTG AAGAAAAATGTTGACGATGCTTTGAAGAATCCAAATGTTACT TCTGTTGAACATGTTATTGTCTTGAAGAGAACTGGTTCTGAT ATTGATTGGCAAGAAGGTAGAGATTTGTGGTGGAGAGATTTG ATTGAAAAAGCTTCTCCAGAACATCAACCTGAAGCTATGAAT GCTGAAGATCCTTTGTTCATTTTGTACACTTCTGGTTCTACTG GTAAGCCTAAGGGTGTTTTGCATACTACTGGTGGTTACTTGG TTTATGCTGCTACTACTTTTAAGTACGTTTTTGATTACCACCCT GGTGATATTTATTGGTGTACTGCTGATGTTGGTTGGGTTACTG GTCATTCTTATTTGTTGTACGGTCCATTGGCTTGTGGTGCTAC TACTTTGATGTTCGAAGGTGTTCCAAACTGGCCTACTCCAGC TAGAATGTGTCAAGTTGTTGATAAACATCAAGTTAACATCTT GTACACTGCTCCAACTGCTATTAGAGCTTTGATGGCTGAAGG TGATAAGGCTATTGAAGGTACTGATAGATCTTCTTTGAGAATT TTGGGTTCTGTTGGTGAACCTATTAATCCAGAAGCTTGGGAA TGGTACTGGAAGAAGATTGGTAAAGAAAAGTGTCCTGTTGT TGATACTTGGTGGCAAACTGAAACTGGTGGTTTCATGATTAC TCCTTTGCCAGGTGCTATTGAATTGAAAGCTGGTTCTGCTAC TAGACCATTTTTCGGTGTTCAACCAGCTTTGGTTGATAATGA AGGTCATCCTCAAGAAGGTGCTACTGAAGGTAACTTGGTTAT TACTGATTCTTGGCCAGGTCAAGCTAGAACTTTGTTCGGTGA TCATGAAAGATTCGAACAAACTTACTTTTCTACTTTCAAGAA CATGTACTTCTCTGGTGATGGTGCTAGAAGAGATGAAGATGG TTATTACTGGATTACTGGTAGAGTTGATGATGTTTTGAATGTT TCTGGTCATAGATTGGGTACTGCTGAAATTGAATCTGCTTTGG TTGCTCATCCAAAAATTGCTGAAGCTGCTGTCGTTGGTATTC

	CTCATGCTATTAAGGGTCAAGCTATTTATGCTTACGTTACTTT GAACCATGGTGAAGAACCTTCTCCTGAATTGTATGCTGAAGT TAGAAACTGGGTTAGAAAGGAAATTGGTCCTTTGGCTACTCC AGATGTTTTGCATTGGACTGATTCTTTGCCAAAAACTAGATCT GGTAAGATTATGAGAAGAATTTTGAGAAAGATCGCTGCTGGT GATACTTCTAACTTGGGTGATACTTCCACTTTGGCTGATCCAG GTGTTGTTGAAAAACCTTTGGAAGAAAAGCAAGCTATTGCT ATGCCTTCTTAA
ACC1(S1132A)	atgagtagtgttaaccactctctccgtcattcaaagctaccgccgcatttccttggtctcaactcggttg aagtcgctgctccctccaaggtcagagactttgtcagggaccatggtggccactcggtcatcacga gagtgctgatcgcaaacaacggtatagctgccgtgaaagaaattcgttccgtcaggaaatgggcgt atgaaacgtttggtaacgatagagccattcaatttattgttatggctaccccagaggatcttgaagcta atgctgaatatattcgaatggctgaccagtatgtcatggtcccaggaggaactgcaaacaacaactat gcgaacgtcgacctcattgtagaaatagcagaatctactgatgctcatgctgtttgggctggttgggg ttttgcctccgaaaatccccatttgcctgagcaactggccgcttctcctaagaagattatcttcattggc cctccgggctctgccatgcgatctcttggtgacaagatttcctctactattgtcgcacaacatgctaaa gtcccatgtattccttggtcaggaactggtgtcgatcaggttataatcgaccccgtaagcaatttggttt ccgttgatgaagaaacgtacgccaaaggatgctgttccgatccacaggacggtttggcaaaagcca aggctattggtttccctgtgatgattaaagcttccgaaggtggtggtggtaaaggaattagaaaagtt gacagggaggaagattttctttctctttatgatcaagctgctaatgaaattccaggttccccaatttttatc atgaagcttgctggagatgccaggcatttggaagttcaattacttgctgatcaatatggaaccaacatc tccctttttggaagagattgttccgttcaaagaagacaccaaaagatcatagaagaggcaccagttac cattgccaaacaagacactttcaggcaaatggaacaagccgctgtcagactgggtcaattggttgga tacgtttctgccggtaccgttgagtatctatattcacacgctgaggacaagttctacttcttggaactga accctcgtcttcaagttgagcatccaaccacagaaatggccacaggtgtcaatcttccagttgccca gttgctaattgcaatgggtattcctttgaatagaatcagagatatcagggtactttacggacttgaacca aatggcgctacagaaattgactttgaattcaaaactgaagaaagcttgaagagtcaaagaaaacccca ttccaaagggtcacactattgcatgtcgtatcacatctgaagatcctggtgaaggttttaagccttctgg tggtgctctatatgagctaaatttcagatcttcttctagcgtttggggttacttcagtgtaggaaacaaat cctcaattcattctttcagtgactctcaatttggtcatatattctcgtttggcgaaaaccgtcaaatcgcca gaaaaaatatggtcgtcgccttgaaagagctttctattcgtggtgactttagaactacaattgagtactt aataaaactgttggaaacagctgatttcgagaacaacaccatcactactggttggttggacgaactga tctcgaagaagctgactgctgaaagacctgatgaaaccacagcaattttatgtggtgctgaaaaagg tcaaatcccaggcaaagaacttcttcgtactattttcccaattgaatttatttatgaaggaaagaagtac aagtttactgtggttcaggctgcatttgacaaatacaacgtctttgtcaacggatgtatgattactgtaa gtgtaacccatttgaaggatggcagtttattggtagcacttgatggtaaatcccattctgtctattacttg caggaagaagtcggaaatactaggttgtcggtggatggtaaatcttgcattttagaagttgagcatga gccaactgaacttcgtactccatctccaggtaaacttatcaaatatcttgtggaacacggtgatcacgt caaaattggacaaccttacgctgaagttgaagtaatgaagatgtgtatgcctttggtcagtcaggaga atggaactatcaggttattgaagcagccaggatcttcggttgccgctggagacatccttgctattcttg cattggatgatcccagcaaggtgaagcatgctttgccattcgatggtacaatccctgatatgaaacag ccatttatccatagcaacaaaccagtttataagttcatttctcttctctccgtgctgaaaaacattttagca gggtatgataatcaagttgtgatgaacgatactctgcagagtctattggatgtgttgaagaaccctgaa cttccttattcggaatggaatcattcgatatctgcacttcattcaaggttaccaattcatttggacgaaca

	attgaccagtttgattgagagatcgcatcaacgtggtgcagactttccagctaagcacttgctcaagct tttggacaaggagcaggctgttaatcctgatccacttttctcccaggtcattgcgcctcttactgctgtt gccaaaagctacgaacatggacttgaagttcatgaacacaatgtattcgccgatttgatcacccaata ctacgacatagagagcttgtttgccgataaaagggaggaagatgttattttacagctacgtgatgaga acaaatcgtcccttgacaaggtcatcgatgtcgtcttgtcacattccagagttggagctaagaaccatt taatcagagctattctggaaatttatcaaactatctgccaaaatgatctccaagctgcaaccattttgaa gaaacctttgaaaaagattgttgagctagattctagatttacagcaaaggtttcgttaaaagctagaga gattttgattcaatgttcccttccctctatcaaagaacgttcagaccagctcgagcatatccttcgatctt cagttgtacaaactcagtacggagagagcttcaatggaaactacaaactgcctaacttggacgttata caagacgtaattgattccaagtacattgtattcgatgttttgacacaatttgttgttagcccaaacaagta tatatttgcagcagcagccgaggtgtatctgcgaagagcttacagggcttactcggtgagagaagtt aaacatcatttcgtaggtgattctgctctcccaattgtggaatggaagttccaattgccgctgttatcaa cagctgcttacaattccgtgcctgaagctatgagaaactcctccagtaaccgatcctctatttcaatgg atagagcagttgctgtctccgatttgaccttcatgatcaacaagaatgattctcaacctttgagaacag gtatcataattcccacaaaccacttagatgacattgaggagtccttgtcatctgccattgatgtcttccct aaacgtccacgtaacaatggaccagctcctgacagaactaatgtggctcctgagcaacctactaac gtatgcaatgttttcattgccaatgtttctggctacaacagtgaggctgagatcgttgacaagattagca gcgttctttctgagttgaaagacgacctcagggctagtggcgttcgaagagttacctttgtcttggga gacaaggttggaacttatccaaaatactataccttcaaatttccagactattttgaagacgagacaatc cgtcacatagagcctgctcttgcgttccagctggaactaagaagattgtccaatttcaatattaaacct gttccaactgagaatagaaatattcatgtgtatgaggcagttgccaaaaatacttcatgcattgacagg agatttttactaggggtatcatcagaacaagcagaatcagagaggatgtgactatctctgaatacctt atcagcgaagctaatcgtcttatgagtgacattttggacgctcttgagattattgatacctccaacactg atttgaaccatatattcatcaatttctctgctgttttcaatgtcacgccagatgacgttgaagcagcgttc ggtggtttcttagaaaggtttggacgtaggctgtggagactacgtgtttctgctgctgaaatccgtatta tgtgcacggaccctgagactggtatcccattcccacttcgtgctttaattaacaacgtttcaggatacgt tgtgaaatctgaaatgtatcaagaggtgaaaaatgatcatggggaatgggttttcaaaagtcttggtcc tacaccaggttcaatgcaccttagaccaatttcaacaccatacccaaccaaagaatggcttcaacca aaacgttacaaagctcatcttatgggtactacttacgtgtatgatttccctgaattattccgtcaagctac gctctcccaatggaaaaaatactctcctactgcgagagttccttctgatgtgtttgtggccaatgaattg atcgtcgatgattcaggtgaactaactgaagtaagcagagaacccggcgccaacgttgtgggtatg gtggccttcaaggtaaccgcaaaaactcctgagtatccacgcggtcgccatttcatcataattgctaat gatatcaccttcaagatcggatcctttggccctcaagaagatgaatatttcaacaaggccacacaact tgcaagaaaattgggcattcctcgaatttatctgtcagccaactcgggtgctagaattggagttgctga agaacttcttccattattcaaagtagcctggaaggaagaaggtaaaccaagcaagggatttgaatact tatacctcacatcggaagatcttactctattggaaaagtccggaaagtctaacagcgttaccactcaa agaatagttgaagaaggcgaagaacgccacgttataactgccatcattggagctagtgatggactg ggtgttgaatgtctaagaggttccggtttgatcgctggtgctacatctcgggcgtacaaggacatcttc actatcacattggtcacctgtagatctgttggtattggtgcttacttggtcagattgggtcaacgagcca ttcaaattgaaggacaaccaataattttgactggtgcccctgctattaataagttgttgggtagggaagt gtactcttccaacctgcaacttggtggtacccagattatgtacaagaacggtgtttcacacttaaccgc caatgatgatctcgcaggtgtcgaaaagattatggattggttagcttatgtgcctgctaagagaaacat gcctgttcctattttagaatcacttcatgacaaatgggacagagatgtggactataagcctacaagaa atgagccgtacgacgtcagatggatgatcagtggacgtgaaactcctgatggtgagttcgaatctgg

	attgtttgactctgggtccttcactgaaactttgagtggatgggctaaaggtgtagtcgtcggaagag cccgtttaggtggtattcctatgggagtcattggtgttgaaactagagtcacagaaaacctgattccag ctgatcccgccaatccagactcaaccgaaatgatgattcaagaagctggtcaagtctggtaccctaa cagtgccttcaagactgcacaagctatcaacgatttcaacaatggtgaacagctacccttgatgatttt ggccaactggagaggtttctctggtggtcaaagagacatgtacaatgaagttttgaaatacggttcttt cattgtggatgctttagtcgacttcaagcagcctatcttcacttacattcctcccactgctgagttgaga ggtggatcttgggttgttgtagaccctaccatcaatgaagacatgatggaaatgtatgcagacgtcga atcaagagcaggtgttttggaaccagaaggtatggtaggtatcaaataccgtaaggacaaactcctt gctactatggaacgattggatgccaaatatgctgagcttaaatccaaggttagcgatactagtctttca gaaaaggatgtttccgagatcaagaaacaaattgagcagagagagaagcaattgttgccaatttatg cacaaatctctattcaatttgctgatcttcatgacagatctggtcgtatgttggccaagggtgtcattaaa aaggaactggaatgggttaattctcgtcgtttcttcttctggagagtccgtcgtcgtttgaacgaggaa tacctcattaagcgtattaccgaattcctatctgcttctgctaccagattggacaagatctcgaggatca attcttggttgccaacatcgattgatttggaagatgaccagaaggttgccatttggttggaagaaaacc gtaaagctcttgacgccaatatcaaggagctcagggctgagcatgttagaagaactctggctactctt gtcagaactgatatggatactacttccaagagtttggctgaattgatcaaccttcttcctgaaaccgaa aaggaatcaattttatctaagatcaagtcatag
POS5	ATGTCTACTTTGGATTCTCACTCTTTGAAATTGCAATCTGGTT CTAAGTTTGTTAAGATTAAGCCTGTTAACAACTTGAGATCTTC TTCTTCTGCTGATTTTGTTTCTCCACCAAATTCTAAATTGCAA TCCTTGATTTGGCAAAATCCATTGCAAAATGTTTACATTACCA AGAAGCCATGGACTCCTTCTACTAGAGAAGCTATGGTTGAAT TTATTACTCATTTGCATGAGTCTTACCCTGAAGTTAATGTTATT GTTCAACCTGATGTTGCTGAAGAAATTTCTCAAGATTTCAAA TCTCCATTGGAAAACGATCCAAACAGACCACATATTTTGTATA CTGGTCCAGAACAAGATATTGTTAATAGAACTGATCTGTTGG TTACTTTGGGTGGTGATGGTACTATTTTGCATGGTGTTTCTAT GTTTGGTAACACTCAAGTTCCTCCAGTTTTGGCTTTTGCTTTG GGTACTTTGGGTTTTTTGTCTCCTTTCGATTTCAAGGAACATA AGAAAGTTTTCCAAGAAGTTATCTCTTCTAGAGCTAAGTGTT TGCATAGAACTAGATTGGAATGTCATTTGAAAAAGAAGGATT CTAACTCTTCTATCGTTACTCATGCTATGAACGATATTTTCTTG CATAGAGGTAACTCTCCTCATTTGACTAATTTGGATATTTTCAT

	CGACGGTGAATTTTTGACTAGAACTACTGCTGATGGTGTTGC TTTGGCTACTCCTACTGGTTCTACTGCTTATTCTTTGTCTGCT GGTGGTTCTATTGTTTCTCCATTGGTTCCAGCTATTTTGATGA CTCCAATTTGTCCAAGATCTTTGTCTTTTAGACCTTTGATTTT GCCTCATTCTTCTCATATTAGAATCAAAATCGGTTCTAAGTTG AACCAAAAACCTGTTAACTCTGTTGTTAAGTTGTCTGTTGAT GGTATTCCACAACAAGATTTGGATGTTGGTGATGAAATTTAC GTTATTAACGAAGTTGGTACTATCTATATCGATGGTACTCAATT GCCTACTACTAGAAAGACTGAAAATGATTTCAACAACTCTAA GAAGCCAAAAAGATCTGGTATTTACTGTGTTGCTAAAACTGA AAACGATTGGATTAGAGGTATTAACGAATTGTTGGGTTTTAAT TCTTCCTTCAGATTGACTAAGAGACAAACTGATAACGATTAA

Supplementary Table S6. SgRNA sequences and genomic integration sites used in this study

Targeted Sites	gRNA sequence (5′-3′)
Int1	TATCTGAAGTATTTACTGGG
Int10	AATTACTTCGGGAATAATGG
Int11	TATTAAAAAAGACGATCCCG
Int21	GCACCATCTGGATAGCATTG
Int31	agacacagaagagaactggg
Int32	gtgacgaaagagatgaggtg
Int56	gaaatgttgctcggtgcgcg
Int57	actagggtacagaatttgtg
Int59	aatgatgtcaatcccatacg

Supplementary Table S7. Reference genomes used for transcriptomic analysis of six different strains

Strains	Reference genomes
Komagataella phaffii GS115	https://www.ncbi.nlm.nih.gov/datasets/genome/GCF_000027005.1/
Saccharomyces cerevisiae BY4741	https://www.ncbi.nlm.nih.gov/datasets/genome/GCF_000146045.2/
Ogataea polymorpha NCYC495	https://mycocosm.jgi.doe.gov/Hanpo2/Hanpo2.home.html
Rhodotorula toruloides NP11	https://www.ncbi.nlm.nih.gov/datasets/genome/GCF_000320785.1/
Saccharomyces cerevisiae CEN.PK2-1C	https://www.ncbi.nlm.nih.gov/datasets/genome/GCA_000269885.1/
Yarrowia lipolytica PO1f	https://mycocosm.jgi.doe.gov/YarliW29/YarliW29.home.html

Supplementary Table S8. Comparison of kinetic parameters of ACS activity among different microorganisms

Origin	Substrate	K_m (mM)	K_{cat} (s^{-1})	K_{cat}/K_m ($mM^{-1}s^{-1}$)	V_{max} (μmol min^{-1} mg^{-1})	References
Salmonella enterica ACSwt	acetate	6.047 ± 1.024	276.8 ± 21	45 ± 8	≈ 280	[8]
Bacillus subtilis ACSwt	acetate	0.43	2.53	5.88	2.167	[9]
Methanothrix soehngenii ACSwt	acetate	0.86	66.9	77.79	55	[10]
E. coli ACSwt	acetate	0.20	1.04	5.2	-	[11,12]
P. pastoris ACS1wt	acetate	0.111 ± 0.010	47.29 ± 1.063	426.057± 39.56	38.397±0.863	This study
P. pastoris ACS1(I658P)	acetate	0.107 ± 0.009	56.34 ± 1.213	526.521± 45.72	45.741±0.985	This study

Supplementary Table S9. Design of ^{13}C isotope-tracing experiments for 3-HP biosynthesis

Group	Ethanol	$NaHCO_3$	Final ethanol concentration	Final $NaHCO_3$ concentration	Experimental purpose
A	Unlabelled ethanol	Unlabelled $NaHCO_3$	100 mM	30 mM	Unlabelled control for baseline isotopologue distribution
B	[U-$^{13}C_2$] ethanol	Unlabelled $NaHCO_3$	100 mM	30 mM	Determine incorporation of the ethanol-derived C_2 unit into 3-HP
C	Unlabelled ethanol	$NaH^{13}CO_3$	100 mM	30 mM	Determine incorporation of inorganic carbon into 3-HP
D	[U-$^{13}C_2$] ethanol	$NaH^{13}CO_3$	100 mM	30 mM	Evaluate simultaneous incorporation of ethanol-derived and inorganic carbon into 3-HP
E	Unlabelled ethanol	None	100 mM	0 mM	Bicarbonate-free control for endogenous inorganic-carbon incorporation
F	[U-$^{13}C_2$] ethanol	None	100 mM	0 mM	Assess whether ethanol-derived carbon can be oxidized to CO_2 and subsequently reincorporated into 3-HP in the absence of exogenous bicarbonate

Common conditions: 150 OD_{600} units of LT-28 cells, 5 mL final reaction volume, 50 mM KPi buffer, 25 °C, 200 rpm.

Supplementary Table S10. Comparison of representative microbial platforms for high-titer 3-HP production

Host organism	Carbon source	Biosynthetic route	Maximum 3-HP titer (g/L)	Reference
K. phaffii	Methanol	Methanol → acetyl-CoA → malonyl-CoA → malonate semialdehyde → 3-HP	48.2	[13]
K. phaffii	Methanol	Methanol → pyruvate → oxaloacetate → aspartate → β-alanine → malonate semialdehyde → 3-HP	42.7	[14]
Corynebacterium glutamicum	Glucose	Glucose → dihydroxyacetone phosphate (DHAP) → glycerol 3-phosphate (G3P) → glycerol → 3-hydroxypropanal (3-HPA) → 3-HP	62.6	[15]
Lentilactobacillus diolivorans	Glycerol + glucose	Glycerol → 3-HPA → 3-HP	67.7	[16]
Rhodosporidium toruloides	Corn stover hydrolysate (glucose + xylose + arabinose)	Glucose → acetyl-CoA → malonyl-CoA → malonate semialdehyde → 3-HP	69.4	[17]
S. cerevisiae	Glucose	Glucose → acetyl-CoA → malonyl-CoA → malonate semialdehyde → 3-HP	71.09	[18]
E. coli	Glycerol	Glycerol → 3-HPA→ 3-HP	77.34	[19]
Ogataea polymorpha	Glucose + xylose	Glucose/xylose → acetyl-CoA → malonyl-CoA → 3-HP	79.6	[20]
Issatchenkia orientalis	Glucose	Glucose → β-alanine → malonate semialdehyde → 3-HP	92.0	[21]
Y. lipolytica	Glucose	Glucose → acetyl-CoA → malonyl-CoA → malonate semialdehyde→ 3-HP	100.37	[22]
Klebsiella pneumoniae	Glycerol	Glycerol → 3-HPA → 3-HP	110.70	[23]
K. phaffii	Ethanol	Ethanol→ acetyl-CoA → malonyl-CoA → malonate semialdehyde → 3-HP	127.04	This study

Supplementary Table S11. The biohybrid systems integrating chemical CO_2 or CO reduction with biological synthesis to produce value-added products

Intermediate	Product	Microorganism	Productivity	References
Ethanol, Acetate (C2)	Lipids	*Rhodococcus jostii* RHA1	<0.08 g/L/h lipid	[24]
Acetic Acid (C2)	Glucose, Fatty Acids	*S. cerevisiae*	<0.01 g/L/h glucose	[25]
Acetic Acid (C2)	Biomass	Yeast, Algae, Mushroom	<0.01 g/L/h biomass	[26]
Ethanol, Acetate (C2)	PHA (C8-C12)	*Pseudomonas putida*	<0.02 g/L/h PHA	[27]
Ethanol, Acetate (C2)	Tyrosine	*E. coli*	<0.005 g/L/h tyrosine	[28]
Acetate (C2)	PHB (C4)	*Ralstonia eutropha*	<0.005 g/L/h PHB	[29]
Formate (C1)	PHB (C4)	*Cupriavidus necator*	<0.005 g/L/h PHB	[30]
Methane (CH4)	Ectoine (C6)	*Methylomicrobium alcaliphilum*	<0.05 g/L/h	[31]
Ethanol (C2)	3-HP (C3)	*K. phaffii* GS115	0.208 g/L/h overall	This study

Supplementary Table S12. Assumptions for the 3-HP production from CO_2-derived ethanol

Parameter	Assumption	References
CO_2 inflow	24,205 kg/h	Aspen plus
CO_2 to Ethanol efficiency	26.1%	This study
Ethanol Selectivity	25.4%	This study
Ethanol production reaction condition	320 ℃, 3 Mpa	This study
3-HP yield	127 g/L	This study
3-HP productivity	0.81 g/(L·h)	This study
Biocatalytic temperature	30 ℃	This study
Biocatalytic pH	5.6	This study
Molar yield of 3-HP from ethanol	13.0%	This study
Biomass yield on O_2	0.753%	This study
Nominal volume of bioreactors	300 m^3	Aspen plus
Total working fermentation volume	950 m^3	Aspen plus
Bioreactor required	4	Aspen plus
Cell-removal recovery	100%	[1]
Activated-carbon recovery	90.4%	[1]
Cation-exchange recovery	93.2%	[1]
Anion-exchange recovery	92.7%	[1]
3-HP overall recovery rate	78.1%	[1]
Final product	30% (w/v) 3-HPsolution	[1]
Annual production capacity of 3-HP	5000 t	Aspen plus

Supplementary Table S13. n^{th}-plant assumptions required by techno-economic analysis[4,32]

Assumption	**Parameters**
Cost year for analysis	2024
Equity for plant	50%
Loan interest and terms	5% annually / 10 years
General plant depreciation period	7 years
Bioreactors depreciation period	10 years
Construction period	2.5 years
Start-up time	0.5 years
Revenues during startup	50%
Variable costs during startup	75%
Fixed costs during startup	100%
Internal rate of return	10%
Income tax rate	21%
Annual operating time	333 day/year (8000 hours/year)
Design years	30 years
Inside battery limit (ISBL)	A100, A200, A300, A400, A500
Warehouse	4% of ISBL
Site development	9% of ISBL
Additional piping	4.5% of ISBL
Indirect costs	**percentage of total direct costs**
Prorateable expenses	10%
Field expenses	10%
Home office and construction fee	20%
Project contingency	10%
Other costs (Start-Up, Permits, etc.)	10%
Fixed operating costs	**percentage of total direct costs**
Employees	13 positions
Labor burden	60% of total salaries
Maintenance	2% of ISBL
Insurance and taxes	0.5% of fixed capital investment

Supplementary Table S14. Capital expenditures for the annual production of 5,000-ton 3-HP from CO_2

Category		Classification	Items	Investment	Total investment
FCI	TDC	Equipment & installation	A100	12.00 MM$	44.54 MM$
			A200	7.39 MM$	
			A300	4.35 MM$	
			A400	10.32 MM$	
			A500	6.32 MM$	
		Warehouse		0.95 MM$	
		Site development		2.14 MM$	
		Additional piping		1.07 MM$	
	TIC	Prorated expenses		4.45 MM$	26.70 MM$
		Field expenses		4.45 MM$	
		Office & construction fee		8.90 MM$	
		Project contingency		4.45 MM$	
		Other costs (Start-Up, permits, etc.)		4.45 MM$	
Land				0.73 MM$	
Working capital				3.65 MM$	
Total capital cost			75.62 MM$		

Supplementary Table S15. Operating expenditures for the annual production of 5,000-ton 3-HP from CO_2

Classification	Items	Investment	Annually costs
Raw material	CO_2 from capture	4.60 MM$/yr	8.75 MM$/yr
	H_2	1.62 MM$/yr	
	Makeup water	0.29 MM$/yr	
	Packing media	0.09 MM$/yr	
	Solar power	2.15 MM$/yr	
By-product's credit	Single cell protein	-6.23 MM$/yr	-8.43 MM$/yr
	Carbon tax	-2.20 MM$/yr	
Labor	Salaries	1.30 MM$/yr	2.08 MM$/yr
	Labor burden	0.78 MM$/yr	
Others	Maintenance	0.47 MM$/yr	0.83 MM$/yr
	Property insurance	0.36 MM$/yr	
Total operating cost		3.23 MM$/yr	

Supplementary Table S16. Global warming potential for producing 1 kg of 3-HP

Impact category	**GWP (kg CO_2-eq)**
CO_2 from capture	-9.99
CO_2 emission	5.76
Solar power	0.62
Water	0.02
H_2	7.08
Total GWP (kg CO_2-eq)	3.49
By-product	-2.10
3-HP	1.39

Supplementary Table S17. Definitions and evaluation criteria for the substrate comparison in Fig. 1a

Metric	Definition / calculation
Atom economy	Atom economy was qualitatively classified according to the theoretical fraction of substrate carbon retained in the representative assimilation pathway and incorporated into the corresponding CoA-activated intermediate. Higher scores indicate greater carbon incorporation efficiency
Net reducing equivalents	Net reducing equivalents were calculated based on the representative assimilation pathway required to generate one mole of acetyl-CoA, accounting for pathway-associated redox reactions and carbon loss. Positive values indicate net generation of reducing power, whereas negative values indicate a net requirement for reducing power
Electron equivalents (e^- eq.)	Electron equivalents were calculated as the degree of reduction (γ) of each substrate according to: $\gamma=4C+H-2O-3N$ where C, H, O, and N denote the numbers of carbon, hydrogen, oxygen, and nitrogen atoms in the substrate, respectively
Redox compatibility with 3-HP	Redox compatibility with 3-HP was qualitatively assessed by comparing the net reducing power associated with nexus-molecule assimilation with the reducing-power requirement of downstream 3-HP biosynthesis. The representative 3-HP pathway requires approximately two NADPH equivalents. A reducing-power contribution approximately matching this requirement was classified as well balanced; excess reducing power was classified as surplus; insufficient reducing power was classified as deficit
Biocompatibility	Biocompatibility qualitatively reflects compatibility with microbial growth and metabolism, considering substrate toxicity, cellular tolerance, metabolic accessibility, and engineering feasibility.

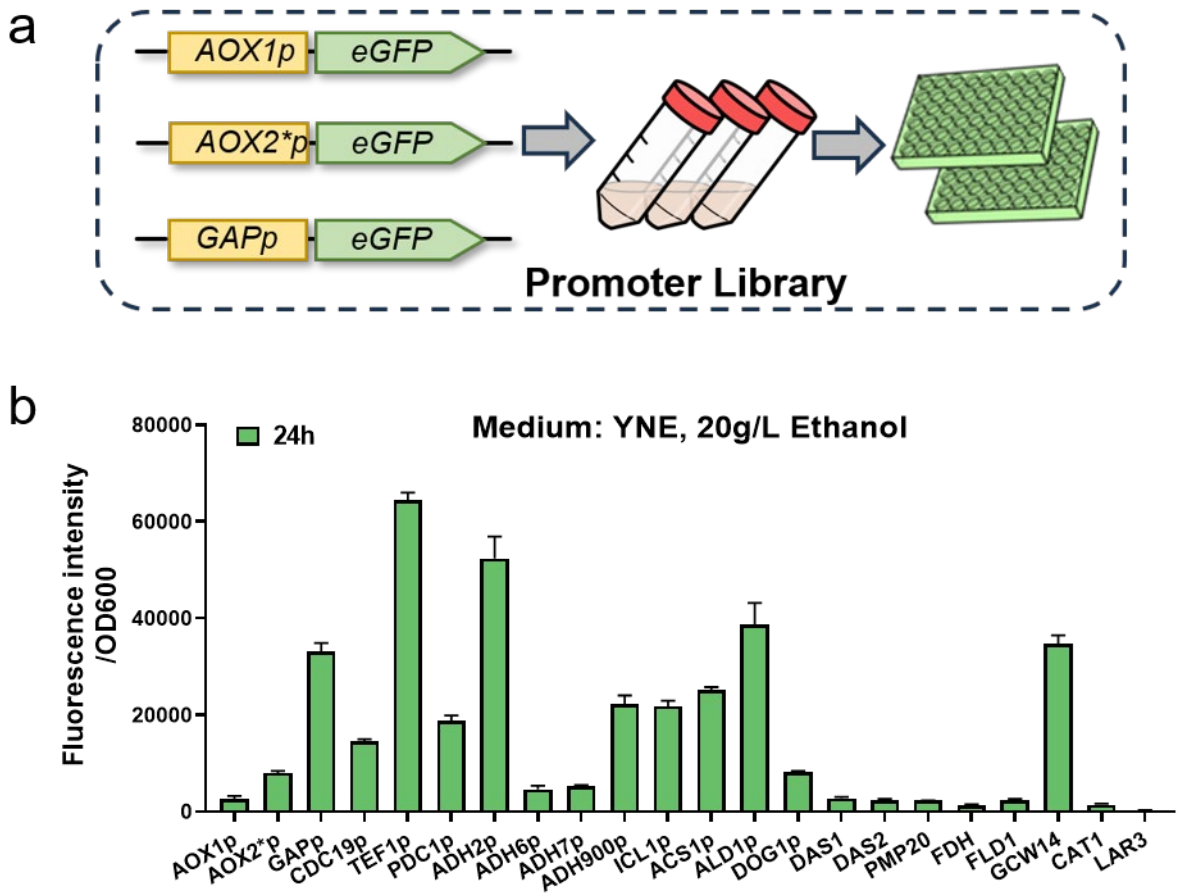

Supplementary Figure S1. Screening of endogenous promoters driving eGFP expression in *K. phaffii* under ethanol-based growth

a, Schematic of the promoter–reporter constructs. A panel of twenty-two endogenous promoters was individually fused to the eGFP reporter upstream of the DUS4t terminator in the HHP backbone, the resulting HHP–promoter–eGFP–DUS4t plasmids were transformed into *K. phaffii* GS115-Cas9 to generate the promoter library.

b, eGFP fluorescence normalized to OD600 in GS115-Cas9 strains harbouring the indicated promoter–eGFP reporters after 24 h of cultivation. Cells were grown in YNE medium containing 20 g/L ethanol in 96-well plates. GFP fluorescence (excitation 488 nm, emission 533 nm) and OD_{600} (600 nm) were recorded on a Tecan Spark multimode microplate reader. Data are presented as the mean ± s.d. of three biological replicates.

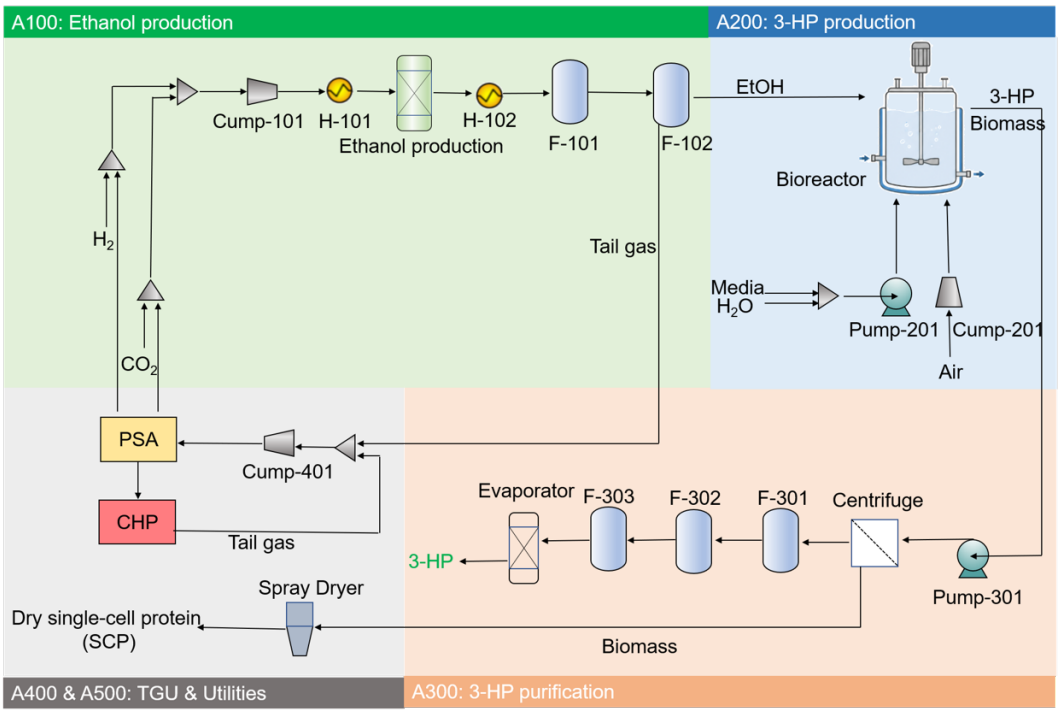

Supplementary Figure S2. Detailed process design for CO_2-derived ethanol conversion to 3-HP

A100, ethanol production; A200, 3-HP production; A300, 3-HP purification; A400–A500, tail-gas treatment and utilities. F-301, activated-carbon treatment; F-302, cation exchange; F-303, anion exchange; PSA, pressure swing adsorption; CHP, combined heat and power; SCP, single-cell protein.

References

1 Mahata, C., Mishra, S. & Singh, V. 3-Hydroxypropionic acid recovery from fermentation broth through novel downstream processing: Technoeconomic analysis. *Bioresource Technology*. **445**, 134094 (2026)

2 Fei, Q. et al. Biological valorization of natural gas for the production of lactic acid: Techno-economic analysis and life cycle assessment. *Biochemical Engineering Journal*. **158**, 107500 (2020)

3 Liu, G., Sun, J., Zhang, J., Tu, Y. & Bao, J. High titer l-lactic acid production from corn stover with minimum wastewater generation and techno-economic evaluation based on Aspen plus modeling. *Bioresource Technology*. **198**, 803-810 (2015)

4 Yu, W. et al. Methanol biotransformation for the production of biodegradable plastic monomer L-lactate in yeast. *Nature Communications*. **16**, 10756 (2025)

5 Ryan Davis, Grundl., N., Tao., L. & Biddy, M. J. Process Design and Economics for the Conversion of Lignocellulosic Biomass to Hydrocarbon Fuels and Coproducts. *Biochemical Design Case Update*. (2018)

6 Kwan, T. H., Hu, Y. & Lin, C. S. K. Techno-economic analysis of a food waste valorisation process for lactic acid, lactide and poly(lactic acid) production. *Journal of Cleaner Production*. **181**, 72-87 (2018)

7 Towler, G. & Sinnott, R. *Chemical Engineering Design: Principles, Practice and Economics of Plant and Process Design*. (Butterworth-Heinemann, 2021).

8 Reger, A. S., Carney, J. M. & Gulick, A. M. Biochemical and Crystallographic Analysis of Substrate Binding and Conformational Changes in Acetyl-CoA Synthetase. *Biochemistry*. **46**, 6536-6546 (2007)

9 Zheng, L. et al. Regulation of acetyl-CoA biosynthesis via an intertwined acetyl-CoA synthetase/acetyltransferase complex. *Nature Communications*. **16**, (2025)

10 Jetten, M. S., Stams, A. J. & Zehnder, A. J. Isolation and characterization of acetyl-coenzyme A synthetase from *Methanothrix soehngenii*. *Journal of Bacteriology*. **171**, (1989)

11 Valgepea, K. et al. Systems biology approach reveals that overflow metabolism of acetate in *Escherichia coli* is triggered by carbon catabolite repression of acetyl-CoA synthetase. *BMC Systems Biology*. **4**, (2010)

12 Walker, M. C., Wen, M., Weeks, A. M. & Chang, M. C. Temporal and fluoride control of secondary metabolism regulates cellular organofluorine biosynthesis. *ACS Chemical Biology*. **7**, (2012)

13 Wu, X. et al. Efficient Bioproduction of 3-Hydroxypropionic Acid from Methanol by a Synthetic Yeast Cell Factory. *ACS Sustainable Chemistry & Engineering*. **11**, 6445-6453 (2023)

14 Covaleda-Cortés, G. et al. Bioprocess intensification for 3-hydroxypropionic acid production from methanol using engineered Komagataella phaffii. *Chemical Engineering Journal Advances*. **26**, 101201 (2026)

15 Chen, Z. et al. Metabolic engineering of Corynebacterium glutamicum for the production of 3-hydroxypropionic acid from glucose and xylose. *Metabolic Engineering*. **39**, 151-158 (2017)

16 Russmayer, H., Ergoth, S., Marx, H. & Sauer, M. Process engineering towards an oxidative cellular state improves 3-hydroxypropionic acid production with Lentilactobacillus diolivorans. *Bioresource Technology*. **382**, 129160 (2023)
17 Hwang, H. J., Adamczyk, P. A., Gladden, J. M. & Liu, D. Inducible flippase-mediated metabolic engineering of Rhodosporidium toruloides for enhanced 3-hydroxypropionic acid production from corn stover hydrolysate. *Bioresource Technology*. **439**, 133368 (2026)
18 Zhang, Y. et al. Engineering yeast mitochondrial metabolism for 3-hydroxypropionate production. *Biotechnology for Biofuels and Bioproducts*. **16**, 64 (2023)
19 Zhang, Y. et al. High-level co-production of 3-hydroxypropionic acid and 1,3-propanediol from glycerol: Metabolic engineering and process optimization. *Bioresource Technology*. **369**, 128438 (2023)
20 Gao, J. et al. Engineering co-utilization of glucose and xylose for chemical overproduction from lignocellulose. *Nature Chemical Biology*. **19**, 1524-1531 (2023)
21 Tan, S.-I. et al. High yield production of 3-hydroxypropionic acid using Issatchenkia orientalis. *Nature Communications*. **17**, 899 (2026)
22 Kang, F. et al. Expanding the genetic toolkit of Yarrowia lipolytica: Dynamic promoter engineering enables high-titer biosynthesis of 3-hydroxypropionic acid. *Bioresource Technology*. **432**, 132656 (2025)
23 Cao, Q.-Y., Xu, H.-Y., Ye, B.-C. & Zhou, Y. Metabolic and fermentation engineering of Klebsiella Pneumoniae for high-level production of 3-hydroxypropionic acid. *Archives of Microbiology*. **207**, 196 (2025)
24 Chen, K. et al. Electro-biodiesel empowered by co-design of microorganism and electrocatalysis. *Joule*. **9**, (2025)
25 Zheng, T. et al. Upcycling CO2 into energy-rich long-chain compounds via electrochemical and metabolic engineering. *Nature Catalysis*. **5**, 388-396 (2022)
26 Hann, E. C. et al. A hybrid inorganic–biological artificial photosynthesis system for energy-efficient food production. *Nature Food*. **3**, 461-471 (2022)
27 Zhang, P. et al. Chem-bio interface design for rapid conversion of CO2 to bioplastics in an integrated system. *Chem*. **8**, 3363-3381 (2022)
28 Fan, L. et al. Blended nexus molecules promote CO_2 to L-tyrosine conversion. *Science Advances*. **10**, eado1352 (2024)
29 Wi, T.-U. et al. Upgrading carbon monoxide to bioplastics via integrated electrochemical reduction and biosynthesis. *Nature Synthesis*. **3**, 1392-1403 (2024)
30 Lim, J., Choi, S. Y., Lee, J. W., Lee, S. Y. & Lee, H. Biohybrid CO_2 electrolysis for the direct synthesis of polyesters from CO_2. *Proceedings of the National Academy of Sciences*. **120**, e2221438120 (2023)
31 Guo, S. et al. Scalable Electro-Biosynthesis of Ectoine from Greenhouse Gases. *Angewandte Chemie International Edition*. **64**, e202415445 (2025)
32 Yan, X. et al. Paradigm of engineering recalcitrant non-model microorganism with dominant metabolic pathway as a biorefinery chassis. *Nature*

Communications. **15**, 10441 (2024)